

RESEARCH

Open Access



# Migration and invasion of cancer stem cells are prevented by low-intensity pulsed ultrasound therapy

Alba Calero<sup>1</sup>, Tamara Fernández-Marcelo<sup>1</sup>, Paulina Sury<sup>1</sup>, Beatriz de Lucas<sup>2</sup> and Beatriz G. Gálvez<sup>1,3\*</sup> 

## Abstract

**Background** Ultrasound is considered a safe and non-invasive tool in regenerative medicine. In particular, low-intensity pulsed ultrasound (LIPUS) has been used in the clinic for more than twenty years for applications in bone healing. It has been demonstrated to be an effective tool to treat different chronic diseases. We sought to evaluate the effects produced by LIPUS on the properties of human breast cancer stem cells (bCSCs).

**Methods** Cells were stimulated using a traditional ultrasound device with the following parameters: 0.05 W/cm<sup>2</sup> with 10% duty cycle, frequency of 3 MHz and 8 pulses.

**Results** At the parameters used, the ultrasound did not directly affect bCSC proliferation, with no evident changes in morphology. In contrast, the ultrasound protocol affected the migration and invasion ability of bCSCs, limiting their capacity to advance while a major affection was detected on their angiogenic properties. LIPUS-treated bCSCs were unable to transform into aggressive metastatic cancer cells, by decreasing their migration and invasion capacity as well as vessel formation. Finally, RNA-seq analysis revealed major changes in gene expression, with 676 differentially expressed genes after LIPUS stimulation, 578 upregulated and 98 downregulated.

**Conclusions** Overall, these results highlight the potential of LIPUS as a promising non-invasive therapy to target bCSCs and attenuate its capacity to drive migration, invasion, angiogenesis and, ultimately, tumor malignancy. Besides, the ability of LIPUS to modulate gene expression points out its capacity to broadly influence the cellular transcriptome. Therefore, the application of LIPUS as an antitumor therapeutic agent targeting bCSCs may offer a promising new approach to treat cancer. In vivo functional experiments will determine in the future the relevance of LIPUS application for the development of metastasis.

**Keywords** Low-intensity pulsed ultrasound, Breast cancer stem cell, Migration, Invasion, Angiogenesis

\*Correspondence:

Beatriz G. Gálvez  
bggalvez@ucm.es

<sup>1</sup>Department of Biochemistry and Molecular Biology, Faculty of Pharmacy, Universidad Complutense de Madrid (UCM), Madrid, Spain

<sup>2</sup>Faculty of Sports Sciences, Universidad Europea de Madrid, Madrid, Spain

<sup>3</sup>CIBER de Diabetes y Enfermedades Metabólicas Asociadas (CIBERDEM), Instituto de Salud Carlos III (ISCIII), Madrid 28029, Spain



© The Author(s) 2025. **Open Access** This article is licensed under a Creative Commons Attribution-NonCommercial-NoDerivatives 4.0 International License, which permits any non-commercial use, sharing, distribution and reproduction in any medium or format, as long as you give appropriate credit to the original author(s) and the source, provide a link to the Creative Commons licence, and indicate if you modified the licensed material. You do not have permission under this licence to share adapted material derived from this article or parts of it. The images or other third party material in this article are included in the article's Creative Commons licence, unless indicated otherwise in a credit line to the material. If material is not included in the article's Creative Commons licence and your intended use is not permitted by statutory regulation or exceeds the permitted use, you will need to obtain permission directly from the copyright holder. To view a copy of this licence, visit <http://creativecommons.org/licenses/by-nc-nd/4.0/>.

## Background

Breast cancer is the most frequently diagnosed cancer and the leading cause of cancer-related deaths among women worldwide. Considering both sexes, it ranks as the fourth most common cause of cancer mortality [1]. The mortality associated with this tumor is closely related to the occurrence of metastasis. In addition to acquiring a plethora of mutations that drive this process, the cells of the tumor microenvironment (TME) play a key role in metastatic dissemination [2, 3]. The TME is composed of tumor cells and a wide variety of non-tumor cells, all embedded in an extracellular matrix. The communication established between the cells of this ecosystem is very complex, involving cell-cell contacts as well as paracrine signaling, including the release of extracellular vesicles [4]. Among the different cell types that make up the breast cancer microenvironment, the presence of mesenchymal stem cells (MSCs) and cancer stem cells has attracted increasing interest due to their contribution to the pathogenesis of this tumor type [5].

MSCs are multipotent progenitor cells that predominantly reside in the bone marrow that can differentiate into cells of different lineages and migrate to various tissues to repair damage. Additionally, the complex secretome of these cells also contributes to tissue repair and regeneration [6].

Besides carrying out these activities, MSCs are also recruited into tumors [7], as tumors have been classically described as “wounds that never heal” [8]+. The homing of MSCs to tumors is dependent on the presence of cytokines, chemokines, and growth factors released by tumor cells [7]. In vitro assays with breast cancer cell lines have demonstrated the existence of a cytokine network, where IL6 released by cancer cells interacts with the IL6R/gp130 receptor expressed on MSCs, promoting its migration. Additionally, in response to IL6, MSCs produce CXCL7, leading to the release of a large number of cytokines by tumor cells [9, 10]. Moreover, the growth factors FGF2 and VEGF, expressed by the MCF-7 and MDA-MB-231 breast cancer cells, have been shown to induce MSC migration [11]. Once MSCs reach the tumor, they participate in the growth and metastasis of breast cancer and in some cases, they become cancer stem cells (CSCs) after suffering mutations, acquiring tumorigenic and metastatic capacities [12]. About their role in promoting metastasis, MSCs release cytokines and chemokines, such as IL-8, TGF- $\beta$ , and IL-6, among others, which promote BCCs migration [13–15]. Moreover, certain MSC-derived signals have also been identified that initiate the EMT transition in BCCs [16]. Additionally, MSCs stimulate the expansion of CSCs [9].

On the other hand, CSCs, a subpopulation of cancer cells with the ability to self-renew and differentiate into various cell types found in tumors, are thought to arise

from normal stem cells or progenitor cells that acquire mutations [17–19]. CSCs are implicated in tumor initiation, progression, metastasis, and recurrence due to their stem-like properties and resistance to conventional therapies [16, 17, 20]. However, CSCs represent a minority subpopulation within malignant tumors, which consist of non-cancerous cells and diverse subpopulations of cancer cells [17]. A key attribute of CSCs is their plasticity, which may help explain the observed diversity of populations in solid tumors [20, 21]. These capabilities enable CSCs to invade normal tissue, promote angiogenesis, evade the immune system, and consequently contribute to tumor progression and disease recurrence even after undergoing cytotoxic treatments such as radiation therapy [18]. Therefore, it is essential to target CSCs within the tumor to prevent relapse. Nevertheless, most of the tumor is composed of non-CSC cells, which have transient proliferation and do not contribute to long-term tumor growth [17].

Based on the aforementioned points, the protumorigenic role of breast cancer stem cells (bCSCs), along with their involvement in drug resistance in breast cancer treatment, underscores the critical importance of identifying therapies specifically targeting this cell type [22]. In this context, ultrasound technology represents a highly promising novel approach for the non-invasive treatment of cancer.

Ultrasound (US) are mechanical waves with frequencies higher than 15 kHz that exert various effects on tissues and cells depending on the acoustic parameters used in their application. For over fifty years, US has been extensively employed in biomedicine, serving as a safe, non-invasive diagnostic tool for real-time imaging without the emission of radiation [23]. Low-intensity pulsed ultrasound (LIPUS) is characterized by the emission of acoustic waves ranging from 1 MHz to 3 MHz in pulsed form and with reduced power. This technique minimizes thermal effects but still allows acoustic energy to reach the target tissue. In recent years, low-intensity pulsed ultrasound has generated growing interest due to its ability to produce therapeutic effects without significantly elevating tissue temperature, making it a safe and cost-effective tool for clinical applications [24]. Thanks to these properties, LIPUS is used as a form of noninvasive physical stimulation, ideal for various therapeutic treatments, such as tissue repair or bone regeneration. In various types of tumors, LIPUS has been shown to induce cancer cell death, both in vitro and in vivo, when specific acoustic parameters are applied. For instance, US has been shown to inhibit the proliferation of T47D breast cancer cells [25]. Furthermore, when combined with a static magnetic field, it has demonstrated the capacity to induce cell cycle arrest and enhance apoptosis in colon and hepatocellular carcinoma cells [26].

Additionally, LIPUS has also demonstrated a beneficial effect by increasing the chemosensitivity of glioma stem cells (GSCs) and inducing apoptosis in human leukemic cells [27, 28].

This technology has the potential to regulate critical biological events, influencing cell survival and growth in a controlled manner. LIPUS has been reported to stimulate hematopoietic stem cell proliferation [29], promote fibroblast migration [30] and inhibit angiogenesis in endothelial cells [31].

Even though its potential to suppress tumor progression, its effects on essential biological parameters in tumors, including the tumor microenvironment cells, such as bCSCs, remain poorly understood. As previously described, these cells play an essential role in tumor initiation, metastasis, and chemotherapy resistance and for this reason, we aimed to study whether LIPUS waves generated by a conventional device at minimal intensity setting can impact the main physiological functions of CSCs in breast cancer.

## Methods

### Cell culture

Human breast cancer stem cells (bCSCs) were acquired from Cell Progen (CA, USA) and were obtained from human biopsies of human breast cancer tissues (Triple Negative: ER, PR and Her 2 Negative). Cells were positive for CD133, CD44, SSEA3/4, Oct4; Tumorigenicity was quantified (<1000 cells) and Alkaline Phosphatase, Aldehyde Dehydrogenase and Telomerase activities were confirmed. bCSCs vial was unfrozen in T25 flask and cultured with complete medium, consisting of Dulbecco's modified Eagles' medium (DMEM) supplemented with

10% fetal bovine serum (both from Sigma-Aldrich, St Louis, MO, USA), 105 U/mL penicillin/streptomycin, 2 mM L-glutamine and 10 mM HEPES (all from Lonza, Basel, Switzerland). Cultures were maintained for several days at 5% CO<sub>2</sub>/95% air atmosphere at 37°C. Cell expansion was performed on p100 culture plates and cells were passaged in ratio 1:5 each three days. Studies were performed using cells from passages 1 to 10 and mycoplasma testing weekly.

### Low-intensity pulsed ultrasound application

Application of ultrasound (therapeutic LIPUS) to cells was performed using the Medisound 3000 device (Globus, Codognè, Italy), which is approved by the EU for use in hospitals and physiotherapy clinics. Unlike high-intensity ultrasound, LIPUS uses low-power mechanical waves (<3 W/cm<sup>2</sup>) with predominantly non-thermal effects, including cavitation, acoustic flow, and mechanical stimulation at the cellular level [32]. bCSCs were seeded in different plates and maintained in the incubator under controlled conditions of 5% CO<sub>2</sub> at 37 °C for 3–4 days to reach sufficient confluence before LIPUS stimulation. The surface of the US device was coated with a specific US gel (Ultrasound Gel, Konix), which allows the maximum propagation of the US wave. Application of LIPUS to bCSCs was performed using the following parameters (Fig. 1): 0.05 W/cm<sup>2</sup> intensity, 3 MHz frequency and 8 pulses (less than 1 min). Final parameters were selected according previous works [33–36]. LIPUS was applied outside the incubator at room temperature, with control cultures treated identically (no LIPUS stimulation). Once the application was completed, the cells were returned to the incubator.

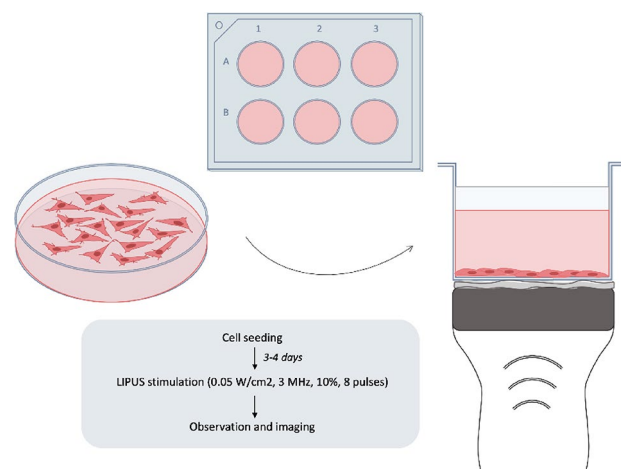


**Fig. 1** Scheme of the LIPUS application and the experimental design. The application of LIPUS was performed with a gel between the transducer and the bottom of the plate where the cells are attached. Ideal LIPUS conditions (0.05 W/cm<sup>2</sup>, 3 MHz, 8 pulses) were applied to a confluent plate of the bCSC line using the Medisound 3000 device, followed by observation and photo-taking. Created by Alba Calero with PowerPoint

### Proliferation assay–bromodeoxyuridine incorporation

The bromodeoxyuridine (BrdU) assay (Merck KGaA, Darmstadt, Germany) was used for proliferation analysis, based on incorporating the thymidine analogue BrdU into DNA strands during replication. Briefly,  $5 \times 10^3$  cells were seeded in each well of a 96-well plate. The next day, BrdU (1:2000 dilution) was added to the culture and cells were maintained for 24 h. Cells were then fixed with 4% paraformaldehyde and washed twice with PBS (Phosphate-Buffered Saline, free of calcium-magnesium, Lonza, Basel, Switzerland). Incorporated BrdU was detected with an anti-BrdU antibody (1:100, 1 h incubation at room temperature), which was visualized with an HRP-conjugated secondary antibody (1:1000, 30 min at room temperature). Finally, after washing twice with PBS, the chromogen substrate was added for 30 min in the dark for the development of the peroxidase reaction. Once the STOP solution was added, the optical density was read in a spectrophotometer (SPECTROstarNano; BMG LABTECH, Aylesbury, UK) at 450 nm.

### Wound-healing assay

To evaluate collective migration, we used the wound-healing assay. Confluent bCSC cultures were scratch wounded with a sterile micropipette tip (size p200). The tip slid across the plate surface to create horizontal and vertical wounds and study the directionality of cell growth. Then, the plate was washed with PBS to remove cellular debris and replenished with complete medium. Cells were maintained in culture and images were captured at different times using a Motic AE31 microscope (Motic, Hong Kong, China). The times studied for wound healing were:  $t_1 = 0$  h;  $t_2 = 8$  h;  $t_3 = 24$  h;  $t_4 = 32$  h;  $t_5 = 48$  h. The measurement and quantification were performed with ImageJ tool and the representation of the images was performed using the PowerPoint. The results were expressed as centimetres of wound closure.

### Invasion assay

Cell invasion was studied with Transwell chambers (COSTAR®) containing 8  $\mu\text{m}$  pore size filters. The day before starting the experiment, the bCSCs line was stimulated with LIPUS (0.05 W/cm<sup>2</sup>, 3 MHz, 8 pulses) for one minute with the ultrasounds probe in contact with the lower side of the chamber. Control and LIPUS-treated bCSCs were plated in 60  $\mu\text{l}$  of the medium in the upper chamber of the Transwell (placed in ECM-coated 24-well plates) and complete culture medium was placed in the lower chamber. They were incubated at different times:  $t_1 = 2$  h,  $t_2 = 4$  h, and  $t_3 = 6$  h. After incubation, chambers were fixed with 4% glutaraldehyde (Sigma-Aldrich) for 2 h and stained with 1% toluidine blue (Sigma-Aldrich) O/N. The top of the filter was wiped with a cotton swab to remove excess cells. Images of the lower side of the membrane were captured in four randomly selected 20X amplitude fields using a Nikon ECLIPSE TE300 fluorescence microscope and cell counting was performed with ImageJ software (Bethesda, MD, USA). The results were expressed as the number of invading cells cell invasions per time.

### Angiogenesis assay

To evaluate the angiogenic activity of bCSCs, we conducted an angiogenesis assay using Matrigel (Corning, Inc.) with reduced growth factors. bCSCs were cultured for 4 days before the experiment and the cells were stimulated with LIPUS (0.05 W/cm<sup>2</sup>, 3 MHz, 8 pulses) the day before the experiment began. DMEM containing 2% FBS Matrigel was applied to 96-well plates (60  $\mu\text{l}$ /well) and incubated for 1 h at 37°C. After that, 50  $\mu\text{l}$  of the control and LIPUS-stimulated bCSCs were incubated on the Matrigel. The number of tubes and tubular networks (panels) was then measured after 2 h by visible light microscopy (Nikon).

### RNA-seq analysis

RNA extraction and sequencing were performed to analyse the gene expression of bCSCs under LIPUS stimulation conditions. bCSCs were cultured for 4 days to reach 80–90% confluence; then, they were stimulated with LIPUS the day before the experiment began. An RNA extraction kit (Invitrogen, ThermoFisher) was used, starting with lysis and homogenization of the cells in monolayer ( $5 \times 10^6$ ) with 0.3–0.6 mL of Lysis Buffer with 2-mercaptoethanol. Subsequently, RNA purification was performed using a binding column and an elution protocol. The concentration and purity of the extracted RNA were measured with a spectrophotometer and its integrity was assessed by agarose gel electrophoresis. The extracted RNA from both control and LIPUS-stimulated bCSCs were sent for sequencing to the Sequencing Department of the Faculty of Pharmacy (UCM). RNA-sequencing library preparation and sequencing of the human bCSCs was carried out by the Genomic Service (UCM, Spain). The Kapa Stranded Total RNA and Ribozero Library Preparation Kit were employed for library construction, and sequencing was performed using the HiSeq 4000 Illumina Platform with 2  $\times$  150 bp paired end reads. The bioinformatics analysis of the generated raw sequence data was carried out using CLC Genomics Workbench 11.0.1. Differential expression was then calculated using multi-factorial statistical analysis based on a negative binomial model that used a generalized linear model approach influenced by the multi-factorial EdgeR method. PCA (Principal Component Analysis) plots were performed for quality control confirming that samples were tightly clustered and experimental samples were also well-separated based on the different treatment. The differentially expressed genes were filtered using standard conditions, an adjusted  $P < 0.05$  and  $|\log_2FC| > 1$ . Microarray data were analyzed using DAVID Analysis software for detection of canonical pathways or tissue's function.

### Statistics

The experiments were observed using a Nikon microscope with different objectives (10X–40X) and the images were captured in the most representative regions of the plates. This allowed us to choose the images used to draw the conclusions of this project. Statistics and graphical representation of the results were performed using GraphPad Prism software (GraphPad Software Inc., San Diego, CA, USA). Between-group comparisons were performed using a two-way analysis of variance (ANOVA) and Šidák's multiple comparisons test. Student's t-test and Mann-Whitney were used when there was only one variable to consider. The analyses performed in each case are highlighted in the Fig. caption. Results were significant when \* $p < 0.05$ ; \*\* $p < 0.01$ ; \*\*\* $p < 0.001$ ; \*\*\*\* $p < 0.0001$ .

## Results

### LIPUS stimulation does not affect bCSC proliferation or cell structure

Prior to experimental testing, a control study was carried out to ensure that the application of LIPUS (Medisound 3000) did not affect cell structure. Exposure to LIPUS (0.05 W/cm<sup>2</sup> and 3 MHz for 8 s; 8 pulses) was performed on attached cells adhered to plates at 80% confluency before experimental testing. As shown in Fig. 2A, cells receiving the ultrasound stimulation were morphologically indistinguishable from control cells. For cell counting experiments,  $1 \times 10^4$  bCSCs were seeded in 24-wells plate and counted over three days by measuring BrdU incorporation. The results were expressed as cell proliferation rate representing the total number of cells present on the plate at the final point (Fig. 2B). LIPUS application under these conditions does not compromise bCSCs integrity or proliferation.

### LIPUS stimulation slows wound healing

To evaluate the impact of LIPUS stimulation on the migratory ability of bCSCs, we conducted a wound-healing assay. We compared control wounded cells with LIPUS-stimulated wounded cells at different time points: t=0 h, t=8 h, t=24 h, t=32 h, and t=48 h (Fig. 3). In the control cells, more than half of the wound had closed by 24 h, and complete closure was achieved by 48 h. In contrast, the LIPUS-stimulated cells exhibited slower healing. It was only at 48 h that healing was almost complete, despite the lower cell density in the wound area compared to the control cells (Fig. 3A). The level of healing was quantified by measuring the intersection space from one end of the wound to the other. A two-way

ANOVA was conducted to analyze the impact of time, treatment, and the interaction between the two factors on wound closure. The results indicated that both time and treatment significantly affect wound closure (Time  $p < 0.0001$ ; LIPUS  $p = 0.006$ ; Time and LIPUS  $p = 0.0063$ ). Wound closure in LIPUS-stimulated cells is slower compared to control cells. This difference is significant at 24 h ( $p = 0.0043$ ) and 32 h ( $p = 0.0006$ ) (Figs. 3B and 3C). These findings suggest that LIPUS stimulation hinders the healing process in bCSCs, indicating a notable impact on the migratory and healing abilities of these cells.

### LIPUS stimulation reduces cell motility and invasion

To assess the impact of LIPUS stimulation on bCSCs' invasiveness, we conducted an invasive migration assay using Transwell chambers at different times: t=2 h, t=4 h and t=6 h (Fig. 4). Cells were placed at the top of the Transwell and those with the ability to invade were retained at the bottom of the filter (Fig. 4B). Control cells were observed to invade faster than LIPUS-stimulated cells at different time points (Fig. 4A). This effect was quantified by counting the number of migrated cells (Fig. 4C). To study the effect of time, treatment, and the interaction between the two factors on cell invasion, a two-way ANOVA was performed. The results showed that time and treatment significantly influence bCSCs' invasiveness (Time  $p < 0.0001$ ; LIPUS  $p = 0.0140$ ; Time and LIPUS  $p = 0.0100$ ). A lower number of migrated cells can be observed in LIPUS-stimulated cells, and this difference was highly significant at 6 h ( $p < 0.0001$ ) (Fig. 4C). These results suggest that LIPUS stimulation decreases cell motility and invasiveness of bCSCs.

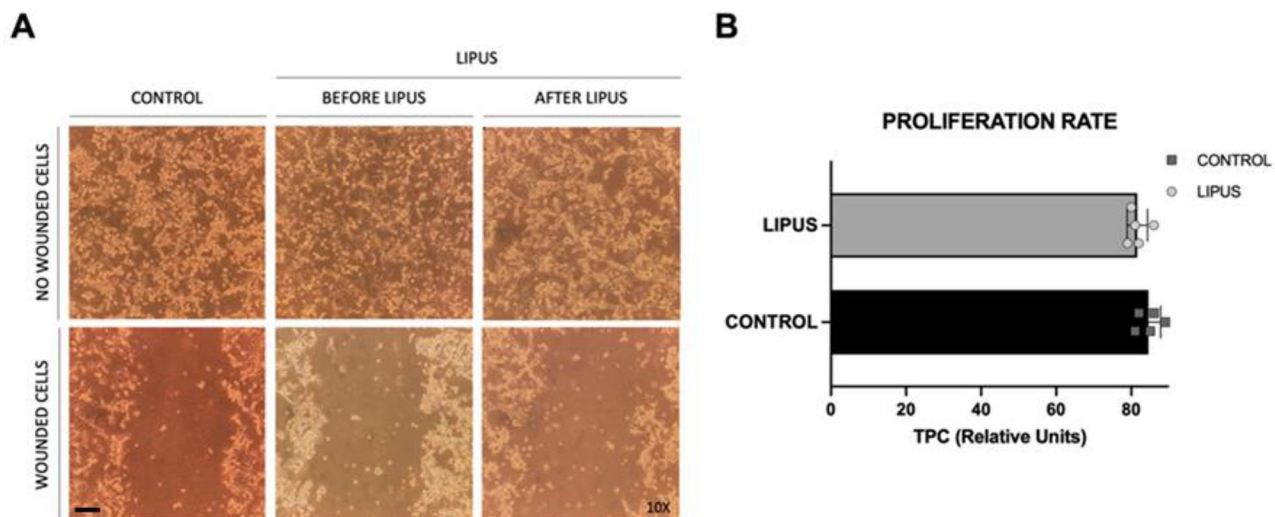


**Fig. 2** LIPUS stimulation does not affect bCSC proliferation or cell structure. **A** Representative images of human bCSCs showing control cells and LIPUS-stimulated cells.  $N=5$ . Bar, 100  $\mu\text{m}$ . **B** bCSC proliferation was evaluated by BrdU incorporation. No significant differences were found between control conditions or treated with LIPUS.  $N=5$

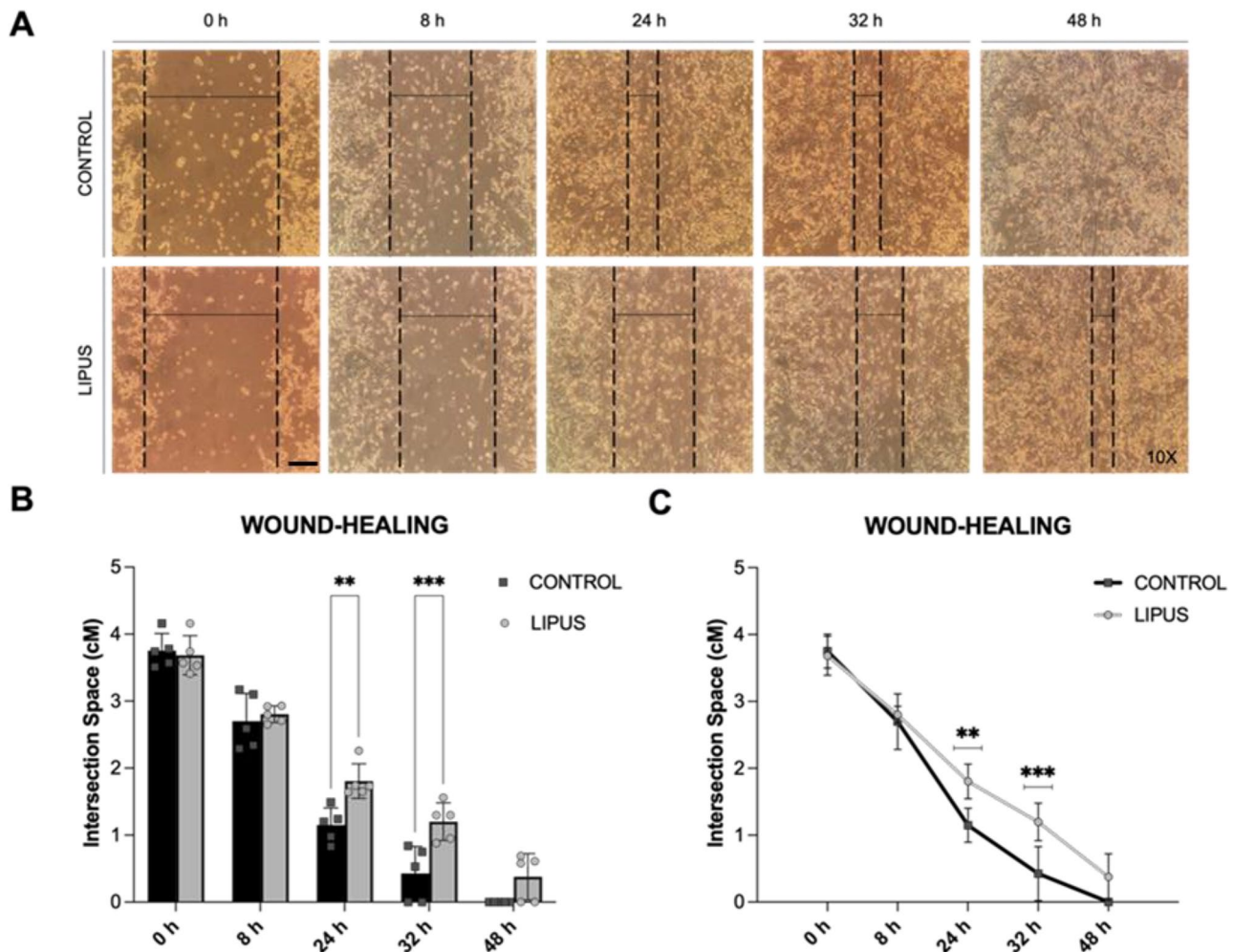


**Fig. 3** LIPUS slows wound closure in bCSCs. **A** Representative images from wounded bCSCs in both control and LIPUS-stimulated conditions (8 pulses, 0.05 W/cm<sup>2</sup> and 3 MHz) at different times (t=0 h, t=8 h, t=24 h, t=32 h and t=48 h). Wound closure is indicated by black dashed lines highlighting the wound edges, and a black horizontal line marks the width of the wound. *N*=5. Bar, 100  $\mu$ m **B-C** Representation of wound closure in both conditions at different times. LIPUS stimulation significantly slows wound closure at 24 and 32 h (determined by two-way ANOVA with Šidák's multiple comparisons test). \*\**p*<0.01; \*\*\**p*<0.001

### LIPUS stimulation decreases angiogenesis

A tube formation assay was conducted on Matrigel to study the impact of LIPUS stimulation on bCSCs' angiogenic activity (Fig. 5). After 2 h, both control and LIPUS-stimulated cells exhibited signs of angiogenesis (Fig. 5A and B). This observation was further confirmed by counting the number of panel-like structures and vessels in both conditions, which were slightly higher in control cells (Fig. 5C). Statistical analysis using Student's *t*-test revealed that LIPUS treatment significantly reduced the formation of new vessels and tubes (*p*=0.0039). These findings suggest that LIPUS stimulation may slow down the formation of panels and vessels, characteristic signs of angiogenesis by bCSCs.

### Gene expression changes induced by LIPUS in human bCSCs

Differentially expressed genes (DEGs) were obtained between control and LIPUS-stimulated samples using an adjusted *P*<0.05 and  $|\log_2FC| > 1$  as cutoffs to define statistically significant differential expression. 676 genes were obtained from which 578 were upregulated when stimulated with LIPUS and 98 genes were subregulated (Supp. Figure 1). To further understand the functions and pathways associated with the differentially expressed genes (DEG), Gene Ontology (GO) and Kyoto Encyclopedia of Genes and Genomes (KEGG) analyses were conducted using the DAVID database [37, 38].

The top 10 DEGs are shown in the volcano plot (Fig. 6A). Of the 10 DEG, all of them were upregulated by ultrasound and 7 genes encoded for proteins belonging to the nucleus (Fig. 6B). Three of these genes codify for

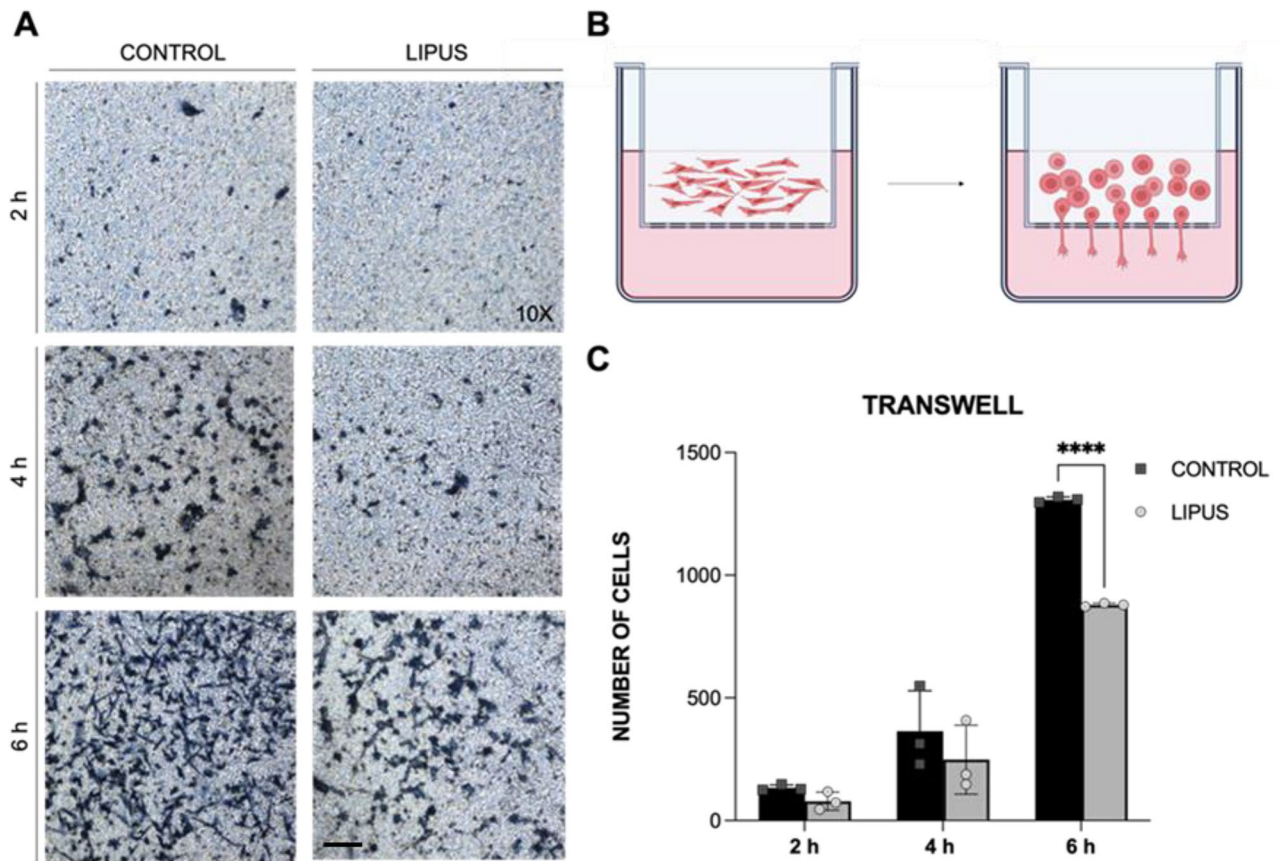


**Fig. 4** LIPUS stimulation reduces bCSC motility and invasion. **A** Representative images taken with a 10X objective of the lower part of the Transwell at different times ( $t=2$  h,  $t=4$  h and  $t=6$  h). Control and LIPUS-stimulated (8 pulses, 0.05 W/cm<sup>2</sup> and 3 MHz) cells have been stained and fixed to analyse the number of migrated cells. Bar, 50  $\mu$ m **B** Representative image of bCSC invasion from the top of the Transwell to the bottom of the filter through the porous membrane. **C** Representation of the number of cells invaded in both conditions at different times. The number of cells that moved through the Transwell is significantly reduced in LIPUS-stimulated cells at 6 h (two-way ANOVA with Šidák's multiple comparisons test). \*\*\*\* $p < 0,0001$ .  $N=3$

histones (H3C15, H3C13 and H3C2) involved in nucleosome assembly and chromatin organization [39, 40]. On the other hand, CEBPD, HES4 and SCAND1 genes encode for transcription factors.

The rest of the upregulated genes were especially enriched for pathways associated with cell differentiation and cell adhesion in the biological process category (Fig. 6C). Among the DEGs associated with differentiation are CCDC85B, HES4, NOTCH1, FOXD3 and SOX15. Other upregulated DEGs of interest are KLF2 and SCAND1.

On the other hand, when categorising the upregulated DEGs by their cellular component, the most significant term is extracellular exosomes, which means that many of the genes in the list encode proteins associated with or found in extracellular exosomes (Fig. 6D). These genes include LAMA5 and IGFBP7. Another significant term is extracellular space, with genes like DcR3 (TNFRSF6B) and MMP21 (Fig. 6D).

Most downregulated genes were associated with or found in the plasma membrane and the membrane

while enriched for pathways related to signal transduction (Fig. 6E and F)). These genes include ANGPT1 and MYCT1. Other downregulated genes were SERPINE2 and LUM (Lumican).

## Discussion

Despite the successful development of new anti-tumor therapies, breast cancer remains one of the most prevalent and challenging cancers worldwide. Relapses in breast cancer are a significant concern, as they indicate the return of cancer after initial treatment [41]. Patients with triple-negative breast cancer (TNBC) suffer from metastasis and relapses more frequently and present worse clinical prognostic [41]. Cancer stem cells although are a minority within the malignant tumor, represent a significant concern due to resistance to conventional radiotherapy and chemotherapy protocols [17]. Other anti-cancer strategies targeting CSCs have been studied in preclinical models [42–44]. However, these strategies are still in development, intending to translate preclinical findings into effective clinical applications.

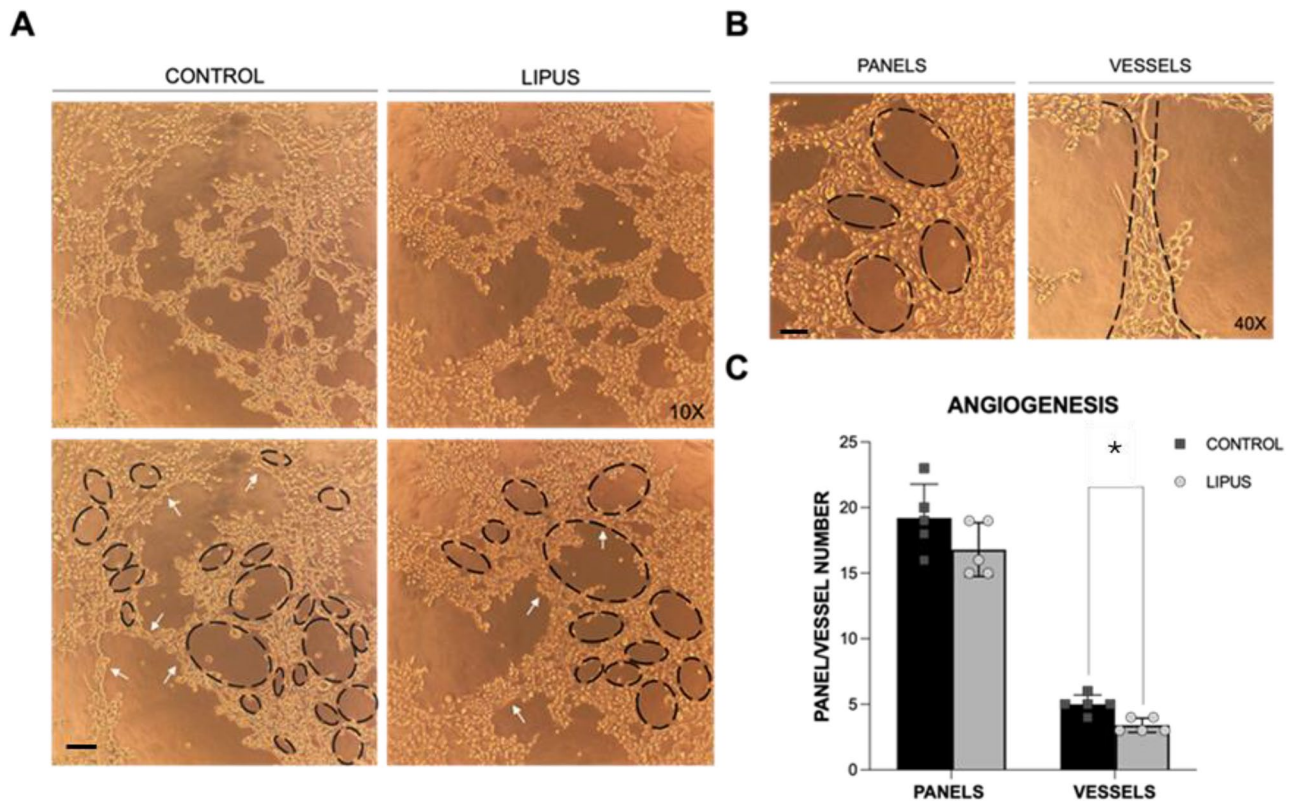


**Fig. 5** LIPUS decreases angiogenesis in bCSCs within 2 h. **A** Images of vessel and tubular network formation (panels) in control and LIPUS-stimulated cells (8 pulses, 0.05 W/cm<sup>2</sup> and 3 MHz) taken with a 10X objective. White arrows indicate vessels and dash black ovals indicate panels. Bar, 100  $\mu$ m **B** Representative images of what have been considered as panels and vessels using a 40X objective. Bar, 50  $\mu$ m **C** Representation of the number of panels and vessels formed in both conditions. Statistical analysis was performed using a Mann-Whitney test. The formation of new vessels and tubes was significantly decreased in LIPUS-treated cells. \*  $p < 0.05$ .  $N = 5$

Understanding the biology of different breast cancer types, and specifically of bCSCs and their response to various treatments, is crucial for developing effective strategies to combat TNBC. This project proposes a new interdisciplinary approach that employs low-intensity pulsed ultrasound, a non-invasive and human-safe tool, which could demonstrate therapeutic efficacy on CSCs.

In the present study, LIPUS intensities of 0.05 W/cm<sup>2</sup> intensity and 3 MHz frequency (8 pulses) were used on human bCSCs, and cell proliferation and structure were analyzed, finding no significant changes between the control and LIPUS-stimulated cells as reported previously in other mesenchymal stem cells models [34]. Therefore, LIPUS stimulation under these conditions does not compromise bCSC integrity or proliferation.

To investigate whether LIPUS stimulation affects the migratory capacity of bCSCs a wound healing assay was performed under LIPUS stimulation. It was observed that LIPUS-stimulated bCSCs took longer to heal the wound, suggesting a reduction in their horizontal migration capacity. While the cells eventually completed the healing process, the slower migration rate implies that LIPUS impairs, but does not completely block, the horizontal

migration of bCSCs. This finding raises the possibility that LIPUS may decrease the ability of these cells to invade adjacent tissues and start the process of metastases. These results also suggested that some of the changes induced by LIPUS take longer to be detected in this type of 2D migration model, possible due to changes in gene expression pattern. To further study this hypothesis, we performed a Transwell invasion assay. The data revealed a reduced number of cells crossing the membrane after LIPUS stimulation, indicating that therapeutic LIPUS slows down cell motility and invasiveness of bCSCs in a 3D model, even at shorter time. These findings were consistent with previous studies showing the effects of LIUS in Ovarian Cancer Stem Cell (OCSC) migration [45], as well as studies showing that LIUS can obstruct the migration of pancreatic tumor cells (Panc-1) [46]. Besides, these results differ from other studies involving a human renal cancer cell line (786-O), a human prostate cancer cell line (PC-3), and a human lung cancer cell line (A549), where LIPUS stimulation did not result in observable changes in their migratory behaviour [47]. Overall, these findings suggest that LIPUS may be a promising therapeutic strategy for modulating bCSCs migration and

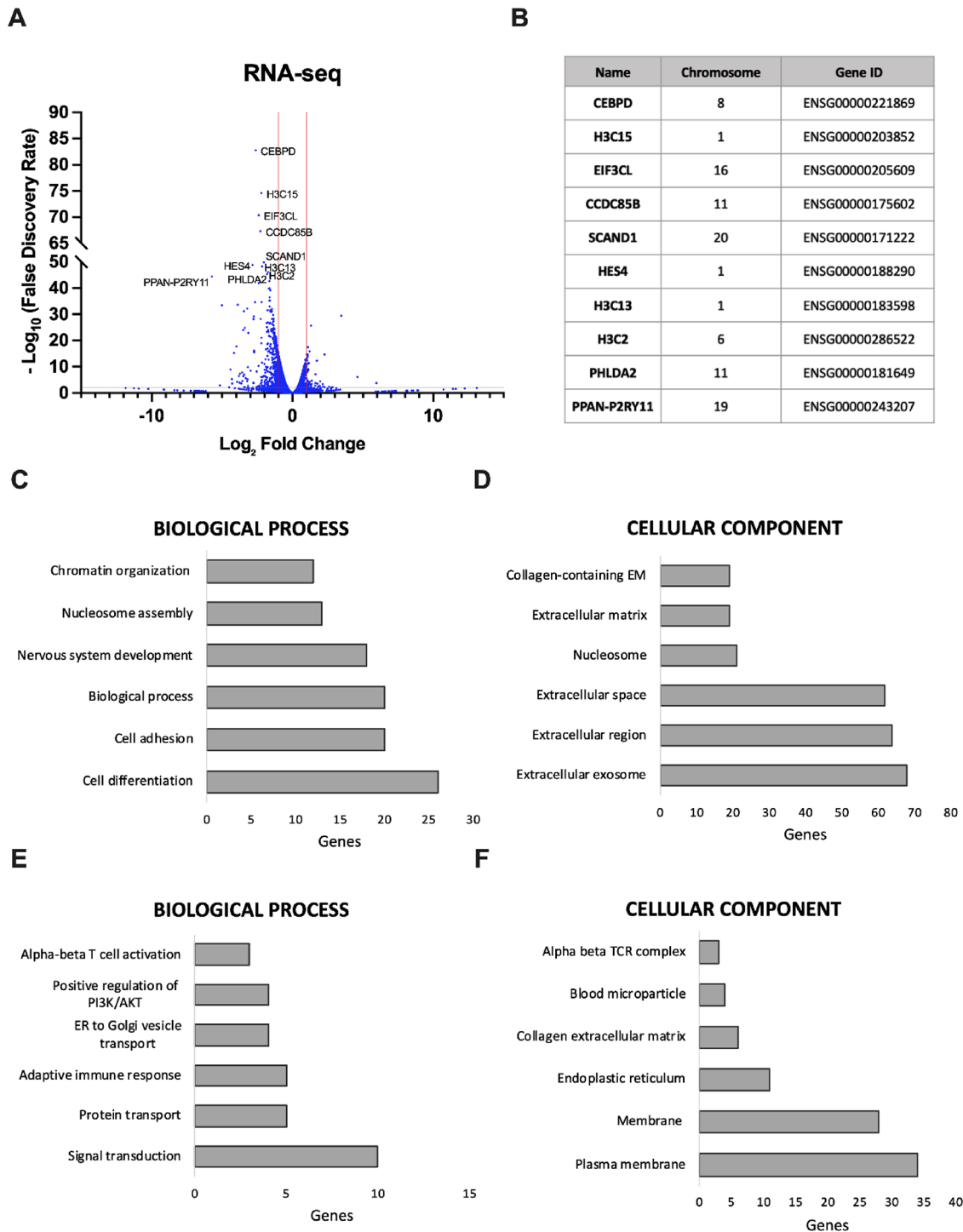


**Fig. 6** RNA-seq Analysis. **A** Volcano Plot showing the top 10 differentially expressed genes between control and LIPUS-stimulated human bCSCs. **B** List of the top 10 differentially expressed genes between control and LIPUS-stimulated human bCSCs. **C-D** Graphical representation of the upregulated DEGs categorized by Biological Process and Cellular Component using Gen Ontology analysis via the David database. **E-F** Graphical representation of the downregulated DEGs categorized by Biological Process and Cellular Component using Gen Ontology analysis via the David database

invasion, two relevant properties for the malignancy, metastasis and recurrence of TNBC.

We next examined whether LIPUS stimulation can influence the angiogenic capacity of bCSCs. This was

assessed using a Matrigel tube formation assay, in which it was observed that LIPUS-stimulated bCSCs formed fewer tubular networks and blood vessels. These observations suggest that LIPUS stimulation may inhibit

angiogenic processes mediated by bCSCs. Consistent with our findings, previous studies have demonstrated that LIPUS may promote apoptosis and inhibit angiogenesis in human umbilical vein endothelial cells (HUVECs) and human microvascular endothelial cells (HMECs) through the p38 signaling pathway [31]. This points to a potential mechanism by which LIPUS could impair angiogenesis and tumor growth. These results deviate from those reported in earlier in vitro studies reporting that LIPUS promotes angiogenesis in endothelial cells (EA.hy926 cell line) by activating the AKT pathway and DNA methylation [48]. This leads us to believe that, although direct studies on LIPUS effects on bCSCs-mediated angiogenesis are limited, LIPUS could impact angiogenesis-related processes in various cell types, including those related to cancer. Further research is required to elucidate the precise mechanisms and the broader implications effects of LIPUS on bCSC-mediated angiogenesis in tumors.

Finally, the RNA-seq analysis revealed that the therapeutic LIPUS caused significant alterations in the gene expression profile of human bCSCs, with 676 genes affected by the treatment. Of these, 578 genes were upregulated, while 98 were downregulated. This transcriptional response highlights the potential of LIPUS to modulate key cellular pathways.

Among the top 10 DEG, seven encoded nuclear proteins, suggesting that LIPUS as a mechanical stimulus can influence nuclear activity.

The upregulated genes were especially enriched for pathways associated with cell differentiation and cell adhesion, both of which are critical to tumor progression and metastasis. Notably, the upregulation of FOXD3, KLF2 and SCAND1 points to the potential of LIPUS. FOXD3 has been reported as a tumor suppressor in breast cancer [49]. This gene is downregulated in breast cancer tissues, and its downregulation is linked to enhanced cell proliferation and invasion via EMT [49]. The overexpression of FOXD3 in response to LIPUS could therefore help suppress tumor growth and metastasis. KLF2, known to inhibit growth, migration, and metastasis in pancreatic ductal adenocarcinoma (PDAC) [50], is similarly downregulated in ovarian tumors, where its re-expression promotes apoptosis and reduces cell growth [51]. Its LIPUS-induced upregulation could exert similar effects in bCSCs. Another upregulated gene is SCAND1, which reverses processes associated with EMT and suppress prostate cancer growth and migration [52].

Conversely, most downregulated genes were enriched for pathways associated with the membrane and the plasma membrane, while enriched for pathways related to signal transduction. Of particular interest were two downregulated genes: ANGPT1 and MYCT1, which play a key role in tumor angiogenesis [53, 54]. Other

downregulated genes were SERPINE2, associated with an aggressive phenotype in the metastasis of many tumors [55, 56]; and LUM, expressed in various cancer tissues and associated with processes such as EMT, cellular proliferation, migration, invasion, and adhesion [57].

Interestingly, some upregulated genes encoded proteins linked to extracellular exosomes and the extracellular space, such as DcR3, MMP21 and LAMA5. Exosomes have been studied in cancer for their role in promoting tumor progression [58]. Some studies identified DcR3 as a key driver of tumor cell migration and invasion [59, 60]. MMP21 was reported to have an important role in the invasion and metastasis process in human colorectal cancer [61], and prior evidence indicated that LAMA5 is promoting the EMT process in ovarian cancer through the Notch signaling pathway [62]. However, the role of exosomes remains complex, as some studies suggest exosomes can also have antitumor properties and contribute to limiting disease progression [58]. When stimulating bCSCs with LIPUS, there was an overexpression of IGFBP7- which has been described as a tumor suppressor in hepatocellular carcinoma [63].

These findings together suggest that LIPUS modulates gene expression of bCSCs to influence critical processes such as apoptosis, angiogenesis, EMT, cell migration and adhesion. By targeting these pathways, LIPUS could be a potential therapeutic tool for limiting bCSCs-driven tumor progression and metastasis. Further research is required to investigate if different LIPUS dosages could target selectively cellular pathways of interests.

## Conclusions

Overall, these results highlight the potential of LIPUS as a promising non-invasive therapy to target bCSCs and attenuate its capacity to drive invasion, angiogenesis and, ultimately, tumor growth and malignancy. The ability of LIPUS to modulate gene expression points out its capacity to broadly influence the cellular transcriptome. Therefore, the application of LIPUS as an antitumor therapeutic agent targeting bCSCs may offer a promising new approach to treat cancer, specifically those more aggressive because of their migration, invasion and angiogenic properties such as TNBC. Future studies will aim to explore additional properties of bCSCs after LIPUS stimulation and translate these findings to in vivo models, which will be essential for examining the direct effects of LIPUS on solid tumors and its potential as a therapeutic intervention.

## Abbreviations

BCCs	Breast Cancer Cells
bCSCs	Breast Cancer Stem Cells
BrdU	Bromodeoxyuridine
CSCs	Cancer Stem Cells
DMEM	Dulbecco's Modified Eagles' Medium
US	Ultrasound

EMT	Epithelial-Mesenchymal Transition
LIPUS	Low-Intensity Pulsed Ultrasound
MSCs	Mesenchymal Stem Cells
TNBC	Triple-Negative Breast Cancer
TME	Tumor Microenvironment

## Supplementary Information

The online version contains supplementary material available at <https://doi.org/10.1186/s12935-025-03854-3>.

Supplementary Material 1: Supplementary Fig. 1: Excel table with the different genes analyzed for RNA-seq. (Worksheet 1) RNA-seq raw data CONTROL vs. LIPUS-stimulated. (Worksheet 2) RNA-seq filtered data for Volcano Plot. (Worksheet 3) RNA-seq filtered data for David Analysis. (Worksheet 4) RNA-seq filtered data for David Analysis, the upregulated genes (Worksheet 5) Gen ontology analysis and graphical representation for the upregulated genes. (Worksheet 6) RNA-seq filtered data for David Analysis, the downregulated genes (Worksheet 7) Gen ontology analysis and graphical representation for the downregulated genes.

## Acknowledgements

The authors would like to acknowledge the collaborative group of CIBER de Diabetes y Enfermedades Metabólicas Asociadas (CIBERDEM), Instituto de Salud Carlos III (ISCIII), 28029 Madrid, Spain.

## Author contributions

A.C.: Methodology; investigation; data curation; formal analysis; visualization; writing—original draft, writing—review & editing. T.F.-M.: Methodology; investigation; writing—original draft. P.S.: Methodology; investigation. B.d.L.: Methodology; investigation; data curation. B. G. G.: Conceptualization; funding acquisition; supervision; writing—original draft, writing—review & editing. All authors approved the final version of the manuscript. The work reported in the paper has been performed by the authors, unless clearly specified in the text.

## Funding

The CNS2022-135241 project assigned to BGG has been financed by MCIN/AEI /<https://doi.org/10.13039/501100011033> and by NextGenerationEU/PRTR. A.C. and T.F.-M. have a contract supported by CNS2022-135241 project.

## Data availability

All data generated or analysed during this study are included in this published article and its supplementary information files.

## Declarations

### Ethics approval and consent to participate

Not applicable.

### Consent for publication

Not applicable.

### Competing interests

The authors declare no competing interests.

Received: 17 January 2025 / Accepted: 10 June 2025

Published online: 14 June 2025

## References

- Bray F, Laversanne M, Sung H, Ferlay J, Siegel RL, Soerjomataram I, et al. Global cancer statistics 2022: GLOBOCAN estimates of incidence and mortality worldwide for 36 cancers in 185 countries. *CA Cancer J Clin*. 2024;74:229–63.
- Liang Y, Zhang H, Song X, Yang Q. Metastatic heterogeneity of breast cancer: Molecular mechanism and potential therapeutic targets. *Semin. Cancer Biol*. Academic Press; 2020. pp. 14–27.
- Riggio AI, Varley KE, Welm AL. The lingering mysteries of metastatic recurrence in breast cancer. *Br J Cancer*. 2021;124:13–26.
- de Visser KE, Joyce JA. The evolving tumor microenvironment: From cancer initiation to metastatic outgrowth. *Cancer Cell*. Cell Press; 2023. pp. 374–403.
- Karnoub AE, Dash AB, Vo AP, Sullivan A, Brooks MW, Bell GW, et al. Mesenchymal stem cells within tumour stroma promote breast cancer metastasis. *Nature*. 2007;449:557–63.
- Tu Z, Karnoub AE. Mesenchymal stem/stromal cells in breast cancer development and management. *Semin Cancer Biol*. 2022;86:81–92.
- Zhang L. The role of mesenchymal stem cells in modulating the breast Cancer microenvironment. *Cell Transpl*. 2023;32.
- Dvorak HF. Tumors: wounds that do not heal. Similarities between tumor stroma generation and wound healing. *N Engl J Med [Internet]*. 1986;315:1650–9. Available from: <http://www.ncbi.nlm.nih.gov/pubmed/3537791>
- Liu S, Ginestier C, Ou SJ, Clouthier SG, Patel SH, Monville F, et al. Breast cancer stem cells are regulated by mesenchymal stem cells through cytokine networks. *Cancer Res*. 2011;71:614–24.
- Rattigan Y, Hsu J-M, Mishra PJ, Glod J, Banerjee D. Interleukin 6 mediated recruitment of mesenchymal stem cells to the hypoxic tumor milieu. *Exp Cell Res*. 2010;316:3417–24.
- Ritter E, Perry A, Yu J, Wang T, Tang L, Bieberich E. Breast cancer cell-derived fibroblast growth factor 2 and vascular endothelial growth factor are chemoattractants for bone marrow stromal stem cells. *Ann Surg*. 2008;247:310–4.
- Bamodu OA, Chung C-C, Pisanic TR, Wu ATH. The intricate interplay between cancer stem cells and cell-of-origin of cancer: implications for therapeutic strategies. *Front Oncol*. 2024;14.
- Kim SH, Bang SH, Kang SY, Park KD, Eom JH, Oh IU, et al. Human amniotic membrane-derived stromal cells (hAMSC) interact depending on breast cancer cell type through secreted molecules. *Tissue Cell*. 2015;47:10–6.
- McAndrews KM, Mcgrail DJ, Ravikummar N, Dawson MR. Mesenchymal stem cells induce directional migration of invasive breast Cancer cells through TGF- $\beta$  OPEN. *Nat Publ Gr [Internet]*. 2015;5:16941. Available from: [www.nature.com/scientificreports](http://www.nature.com/scientificreports).
- De Luca A, Lamura L, Gallo M, Maffia V, Normanno N. Mesenchymal Stem Cell-Derived Interleukin-6 and Vascular Endothelial Growth Factor Promote Breast Cancer Cell Migration. *J Cell Biochem [Internet]*. 2012 [cited 2024 Sep 25];113:3363–70. Available from: <https://onlinelibrary.wiley.com/doi/https://doi.org/10.1002/jcb.24212>
- Martin FT, Dwyer RM, Kelly J, Khan S, Murphy JM, Curran C et al. Potential role of mesenchymal stem cells (MSCs) in the breast tumour microenvironment: stimulation of epithelial to mesenchymal transition (EMT).
- Battle E, Clevers H. Cancer stem cells revisited. *Nat Med*. 2017;23:1124–34.
- Reya T, Morrison SJ, Clarke MF, Weissman IL. Stem cells, cancer, and cancer stem cells. *Nature*. 2001;414:105–11.
- Kreso A, Dick JE. Evolution of the Cancer stem cell model. *Cell Stem Cell*. 2014;14:275–91.
- O'Brien CA, Pollett A, Gallinger S, Dick JE. A human colon cancer cell capable of initiating tumour growth in immunodeficient mice. *Nature*. 2007;445:106–10.
- Bonnet D, Dick JE. Human acute myeloid leukemia is organized as a hierarchy that originates from a primitive hematopoietic cell. *Nat Med*. 1997;3:730–7.
- Zheng Q, Zhang M, Zhou F, Zhang L, Meng X. The breast Cancer stem cells traits and drug resistance. *Front Pharmacol*. 2020;11:599965.
- Sennoga CA, Kanbar E, Auboire L, Dujardin P-A, Fouan D, Escoffre J-M, et al. Microbubble-mediated ultrasound drug-delivery and therapeutic monitoring. *Expert Opin Drug Deliv*. 2017;14:1031–43.
- Diaz-Alejo JF, Gomez IG, Earl J. Ultrasounds in cancer therapy: A summary of their use and unexplored potential. *Oncol Rev*. 2022;16.
- Katiyar A, Osborn J, DasBanerjee M, Zhang LG, Sarkar K, Sarker KP. Inhibition of human breast Cancer cell proliferation by Low-Intensity ultrasound stimulation. *J Ultrasound Med*. 2020;39:2043–52.
- Sengupta S, Khatua C, Pal A, Bodhak S, Balla VK. Influence of ultrasound and magnetic field treatment time on carcinoma cell inhibition with drug carriers: an in vitro study. *Ultrasound Med Biol*. 2020;46:2752–64.
- Lagneaux L, de Meulenaer EC, Delforge A, Dejenneffe M, Massy M, Moerman C, et al. Ultrasonic low-energy treatment: a novel approach to induce apoptosis in human leukemic cells. *Exp Hematol*. 2002;30:1293–301.
- Song S, Ma D, Xu L, Wang Q, Liu L, Tong X, et al. Low-intensity pulsed ultrasound-generated singlet oxygen induces telomere damage leading to glioma stem cell awakening from quiescence. *iScience*. 2022;25:103558.

29. Xu P, Gul-Uludag H, Ang WT, Yang X, Huang M, Marquez-Curtis L, et al. Low-intensity pulsed ultrasound-mediated stimulation of hematopoietic stem/progenitor cell viability, proliferation and differentiation in vitro. *Biotechnol Lett.* 2012;34:1965–73.
30. Atherton P, Lausecker F, Harrison A, Ballestrem C. Low-intensity pulsed ultrasound promotes cell motility through vinculin-controlled Rac1 GTPase activity. *J Cell Sci.* 2017;130:2277–91.
31. Su Z, Xu T, Wang Y, Guo X, Tu J, Zhang D, et al. Low-intensity pulsed ultrasound promotes apoptosis and inhibits angiogenesis via p38 signaling-mediated Endoplasmic reticulum stress in human endothelial cells. *Mol Med Rep.* 2019;19:4645–54.
32. Jiang X, Savchenko O, Li Y, Qi S, Yang T, Zhang W, et al. A review of Low-Intensity pulsed ultrasound for therapeutic applications. *IEEE Trans Biomed Eng.* 2019;66:2704–18.
33. Fernández-Marcelo T, Calero A, de Lucas B, Garrido M, Arregui RL, Sury P et al. Low intensity pulsed ultrasounds modulate adipose stem cells differentiation. *Stem Cell Rev Rep.* 2025.
34. de Lucas B, Pérez LM, Bernal A, Gálvez BG. Application of low-intensity pulsed therapeutic ultrasound on mesenchymal precursors does not affect their cell properties. *PLoS ONE.* 2021;16:e0246261.
35. de Lucas B, Pérez LM, Bernal A, Gálvez BG. Ultrasound Therapy: Experiences and Perspectives for Regenerative Medicine. *Genes (Basel)* [Internet]. 2020;11:1086. Available from: <https://www.mdpi.com/2073-4425/11/9/1086>
36. Bernal A, Pérez LM, De Lucas B, Martín NS, Kadow-Romacker A, Plaza G, et al. Low-Intensity pulsed ultrasound improves the functional properties of cardiac mesoangioblasts. *Stem Cell Rev Rep.* 2015;11:852–65.
37. Huang DW, Sherman BT, Lempicki RA. Systematic and integrative analysis of large gene lists using DAVID bioinformatics resources. *Nat Protoc.* 2009;4:44–57.
38. Sherman BT, Hao M, Qiu J, Jiao X, Baseler MW, Lane HC, et al. DAVID: a web server for functional enrichment analysis and functional annotation of gene lists (2021 update). *Nucleic Acids Res.* 2022;50:W216–21.
39. Kujirai T, Kurumizaka H. Transcription through the nucleosome. *Curr Opin Struct Biol.* 2020;61:42–9.
40. Tachiwana H, Osakabe A, Shiga T, Miya Y, Kimura H, Kagawa W, et al. Structures of human nucleosomes containing major histone H3 variants. *Acta Crystallogr D Biol Crystallogr.* 2011;67:578–83.
41. Won K-A, Spruck C. Triple-negative breast cancer therapy: current and future perspectives (Review). *Int J Oncol.* 2020;57:1245–61.
42. Jin L, Hope KJ, Zhai Q, Smadja-Joffe F, Dick JE. Targeting of CD44 eradicates human acute myeloid leukemic stem cells. *Nat Med.* 2006;12:1167–74.
43. Huang T, Song X, Xu D, Tiek D, Goenka A, Wu B, et al. Stem cell programs in cancer initiation, progression, and therapy resistance. *Theranostics.* *Ivyspring International*; 2020. pp. 8721–43.
44. Lagadinou ED, Sach A, Callahan K, Rossi RM, Neering SJ, Minhajuddin M, et al. BCL-2 Inhibition targets oxidative phosphorylation and selectively eradicates quiescent human leukemia stem cells. *Cell Stem Cell.* 2013;12:329–41.
45. Yang Y, Du M, Yu J, Chen Z. Biomechanical response of Cancer stem cells to Low-Intensity ultrasound. *J Biomech Eng.* 2023;145.
46. González I, Luzuriaga J, Valdivieso A, Candil M, Frutos J, López J, et al. Low-intensity continuous ultrasound to inhibit cancer cell migration. *Front Cell Dev Biol.* 2022;10:842965.
47. Sawai Y, Murata H, Koto K, Matsui T, Horie N, Ashihara E, et al. Effects of low-intensity pulsed ultrasound on osteosarcoma and cancer cells. *Oncol Rep.* 2012;28:481–6.
48. Li J, Guo W, Yu F, Liu L, Wang X, Li L, et al. Low-intensity pulsed ultrasound promotes angiogenesis via the AKT pathway and DNA methylation in human umbilical vein endothelial cells. *Ultrasonics.* 2022;118:106561.
49. Chu T-L, Zhao H-M, Li Y, Chen A-X, Sun X, Ge J. FoxD3 deficiency promotes breast cancer progression by induction of epithelial-mesenchymal transition. *Biochem Biophys Res Commun.* 2014;446:580–4.
50. Zhang D, Dai Y, Cai Y, Suo T, Liu H, Wang Y, et al. KLF2 is downregulated in pancreatic ductal adenocarcinoma and inhibits the growth and migration of cancer cells. *Tumor Biol.* 2016;37:3425–31.
51. Wang F, Zhu Y, Huang Y, McAvoy S, Johnson WB, Cheung TH, et al. Transcriptional repression of WEE1 by Kruppel-like factor 2 is involved in DNA damage-induced apoptosis. *Oncogene.* 2005;24:3875–85.
52. Eguchi T, Cizmadiá E, Kawai H, Sheta M, Yoshida K, Prince TL, et al. SCAND1 reverses Epithelial-to-Mesenchymal transition (EMT) and suppresses prostate Cancer growth and migration. *Cells.* 2022;11:3993.
53. Xu J, Sun Y, Fu W, Fu S. MYCT1 in cancer development: gene structure, regulation, and biological implications for diagnosis and treatment. *Biomed Pharmacother.* 2023;165:115208.
54. METHENY-BARLOW LJ, LI LY. The enigmatic role of angiopoietin-1 in tumor angiogenesis. *Cell Res.* 2003;13:309–17.
55. Zhang S, Jia X, Dai H, Zhu X, Song W, Bian S, et al. SERPINE2 promotes liver cancer metastasis by inhibiting c-Cbl-mediated EGFR ubiquitination and degradation. *Cancer Commun (London England).* 2024;44:384–407.
56. Wang K, Wang B, Xing AY, Xu K, Sen, Li GX, Yu ZH. Prognostic significance of SERPINE2 in gastric cancer and its biological function in SGC7901 cells. *J Cancer Res Clin Oncol.* 2015;141:805–12.
57. Giatagana E-M, Berdiaki A, Tsatsakis A, Tzanakakis GN, Nikitovic D. Lumican in Carcinogenesis-Revisited. *Biomolecules.* 2021;11.
58. Paskeh MDA, Entezari M, Mirzaei S, Zabolian A, Saleki H, Naghdi MJ, et al. Emerging role of exosomes in cancer progression and tumor microenvironment remodeling. *J Hematol Oncol.* 2022;15:83.
59. Weissinger D, Tagscherer KE, Macher-Göppinger S, Haferkamp A, Wagener N, Roth W. The soluble decoy receptor 3 is regulated by a PI3K-dependent mechanism and promotes migration and invasion in renal cell carcinoma. *Mol Cancer.* 2013;12:120.
60. Macher-Goeppinger S, Aulmann S, Wagener N, Funke B, Tagscherer KE, Haferkamp A, et al. Decoy receptor 3 is a prognostic factor in renal cell cancer. *Neoplasia.* 2008;10:1049–56.
61. Huang Y, Li W, Chu D, Zheng J, Ji G, Li M, et al. Overexpression of matrix metalloproteinase-21 is associated with poor overall survival of patients with colorectal cancer. *J Gastrointest Surg.* 2011;15:1188–94.
62. Diao B, Sun C, Yu P, Zhao Z, Yang P. LAMA5 promotes cell proliferation and migration in ovarian cancer by activating Notch signaling pathway. *FASEB J.* 2023;37:e23109.
63. Zhang L, Lian R, Zhao J, Feng X, Ye R, Pan L, et al. IGFBP7 inhibits cell proliferation by suppressing AKT activity and cell cycle progression in thyroid carcinoma. *Cell Biosci.* 2019;9:44.

## Publisher's note

Springer Nature remains neutral with regard to jurisdictional claims in published maps and institutional affiliations.